

K-corrections for Type Ia Supernovae in the CFHT Legacy Survey

Eric Hsiao

September 15, 2003

Abstract. Type Ia supernovae may be used for the determination of cosmological parameters. The CFHT Legacy Survey will discover on the order of thousands of Type Ia supernovae and make precise measurements of the brightness of these objects. The determination of cosmological parameters requires the comparison in brightness of low and high redshift supernovae. Precise K-corrections are needed to account for the effects of redshift. The CFHT Legacy Survey adopts the Sloan Digital Sky Survey (SDSS) photometric system (Fukugita et al. 1996). The SDSS system is drastically different from the traditional Johnson-Cousins photometric system (Johnson & Morgan 1953; Cousins 1978). The goals of this project are to calculate the K-corrections for the SDSS system, using the methods outlined in Nugent et al. (2002), and to develop cross-system and commutable K-corrections between the two photometric systems.

1. Introduction

K-correction deals with the technical effects of redshift z in a supernova spectrum. The need for K-correction arises from the fact that the brightness of a supernova can only be observed through a fixed bandwidth filter. The spectrum of a very distant supernova is stretched and shifted toward longer wavelengths. To compare the brightness of such a supernova to the brightness of a much closer supernova requires the aid of K-corrections of the corresponding filter bands.

For a magnitude observed in a certain band, one can obtain the magnitude of the unshifted and unstretched supernovae spectra in another rest-frame band, with the knowledge of the appropriate cross-filter K-corrections:

$$m_y(t(1+z)) = M_x(t) + K_{xy}(z, t) + \mu(z)$$

K_{xy} denotes the K-correction from the observed y band to the rest-frame x band. The observed magnitude of a supernova is expressed as the sum of its absolute magnitude at rest-frame M_x , the cross-filter K-correction K_{xy} , and the distance modulus μ . K-correction is a function of supernova epoch t and redshift z .

Cross-filter K-correction allows one to correct between different filter bands or between bands of different photometric systems. K_{xy} is defined as follows (Nugent et al. 2002):

$$K_{xy} = -2.5 \log \left(\frac{\int \lambda Z_x(\lambda) S_x(\lambda) d\lambda}{\int \lambda Z_y(\lambda) S_y(\lambda) d\lambda} \right) \quad \text{zero magnitude term} \\ + 2.5 \log(1+z) \quad \text{bandwidth term} \\ + 2.5 \log \left(\frac{\int \lambda F(\lambda) S_x(\lambda) d\lambda}{\int \lambda F(\lambda/(1+z)) S_y(\lambda) d\lambda} \right) \quad \text{selective term}$$

$F(\lambda)$ is the spectral energy distribution at the supernova. $S_x(\lambda)$ and $S_y(\lambda)$ are the effective transmissions of the rest-

frame x and the observed y filter bands respectively. The effective transmissions include the filter transmissions and the detector quantum efficiencies.

$Z_x(\lambda)$ and $Z_y(\lambda)$ are the idealized zero magnitude spectral energy distribution of the rest-frame x and the observed y filter bands respectively. All filter bands in a particular photometric system would yield zero magnitudes when they are used to observe the $Z_x(\lambda)$ and $Z_y(\lambda)$ spectra. For example, $u^*=g'=r'=i'=z'=0$ for $Z_y(\lambda)$, if the observed y band is in the SDSS photometric system. It should be noted that $Z_x(\lambda)$ and $Z_y(\lambda)$ are different spectra only if the x and the y bands are in different photometric systems. The determination of $Z_x(\lambda)$ and $Z_y(\lambda)$ is detailed in section 3.

K-correction consists of three terms: zero magnitude term, bandwidth term, and selective term. The effects of each term are detailed in the following subsections.

It should be noted that the modern definition of cross-filter K-correction does not include the two factors of $(1+z)$ accounting for the “energy” and the “number” effects of redshift (Sandage et al. 1995). The “energy” effect is due to the fact that every photon received is degraded in energy by $(1+z)$. The “number” effect is caused by the dilution in rate of photon arrival due to the stretching of the path length. These two terms are included in the theory via the following relationship between the observed bolometric flux l_{bol} and the absolute bolometric flux L_{bol} (Robertson 1938):

$$l_{bol} = \frac{L_{bol}}{4\pi(R_0 r)^2} \frac{1}{(1+z)^2}$$

K-correction deals strictly with the observational effects of redshift caused by fixed filter bandwidths.

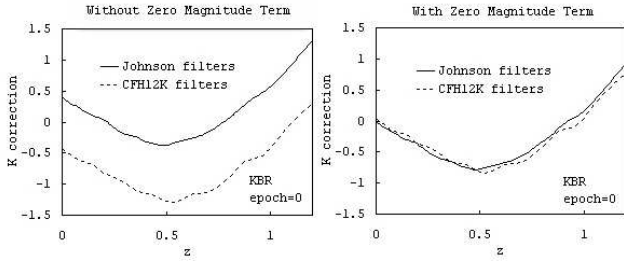


Fig. 1. Effect of the zero magnitude term

1.1. Zero magnitude term

$$-2.5 \log \left(\frac{\int \lambda Z_x(\lambda) S_x(\lambda) d\lambda}{\int \lambda Z_y(\lambda) S_y(\lambda) d\lambda} \right)$$

The zero magnitude term cancels out the magnitude difference between the rest-frame x band and the observed y band at zero magnitudes. The zero magnitude term also eliminates the normalization constant of the effective filter transmissions. The relative transmission amplitudes between filter bands are therefore irrelevant for the purpose of K-correction calculations.

The zero magnitude term is eliminated for a single-filter K-correction, or K_{AA} . However, when the rest-frame x and the observed y bands are different bands in the same photometric system, the zero magnitude term must remain to account for the non-flat zero magnitude spectra in wavelength space.

We can illustrate the effect of the zero magnitude term by comparing the K-corrections of the CFH12K filter set and another typical Johnson filter set. Both filter sets are in the Johnson-Cousins photometric system. For a given light source, the two filter sets should measure the same magnitudes. The K-corrections calculated for the two filter sets should therefore be the same. K-corrections for the CFH12K and the Johnson filter sets are plotted in Figure 1. Without the zero magnitude term, the two K-corrections diverge. With the zero magnitude term, the two K-corrections converge to the desired result.

1.2. Bandwidth term

$$+2.5 \log(1 + z)$$

The bandwidth term corrects for the fact that a stretched supernova spectrum is observed through a fixed bandwidth filter.

This term in the K-correction calculation was originally ignored by Hubble in his galaxy count program (Sandage et al. 1995). The error of excluding the bandwidth term increases with redshift, as shown in Figure 2.

1.3. Selective term

$$+2.5 \log \left(\frac{\int \lambda F(\lambda) S_x(\lambda) d\lambda}{\int \lambda F(\lambda)/(1+z) S_y(\lambda) d\lambda} \right)$$

The selective term accounts for the magnitude difference between the rest-frame x band and the observed y band due to the non-flat supernovae spectra.

Two factors in the selective term dictate the shape of the K-correction in redshift space:

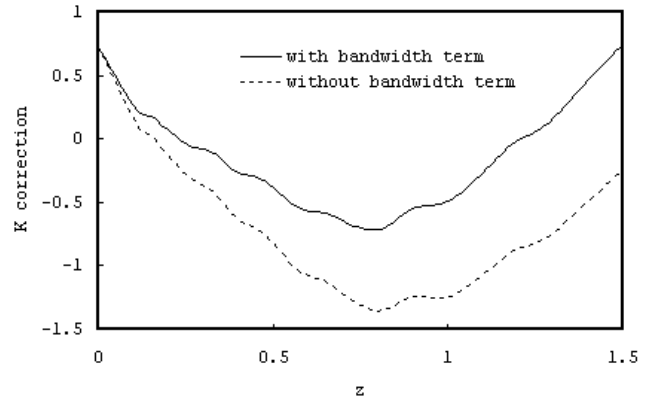


Fig. 2. Effect of the bandwidth term

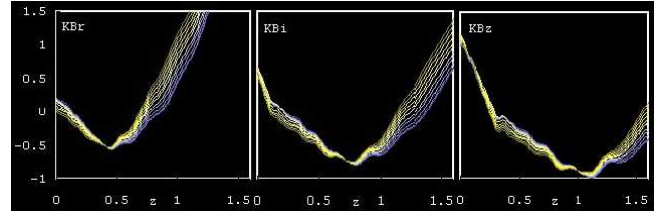


Fig. 3. Effect of the observed y band chosen

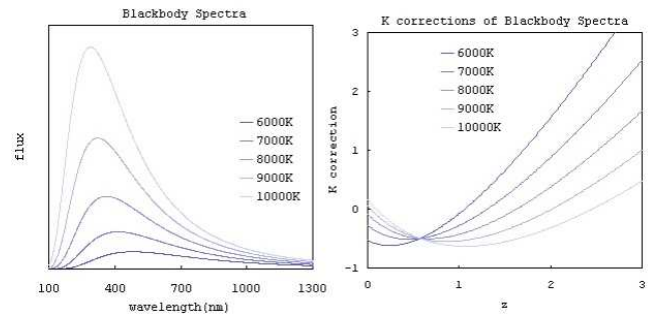


Fig. 4. Effect of the colour of the source spectra

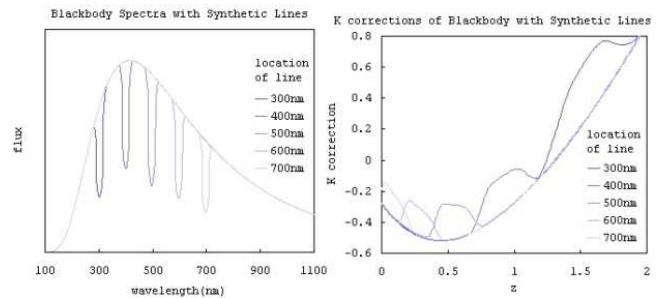


Fig. 5. Effect of lines in the source spectra

1. Observed y band chosen
2. Shape of the supernovae spectra

The observed y band chosen affects the shape of the K-correction in redshift space. Figure 3 compares the shape of the K-corrections $K_{Br'}$, $K_{Bi'}$, and $K_{Bz'}$. Filter bands with longer effective wavelengths yield K-correction minima at higher redshifts.

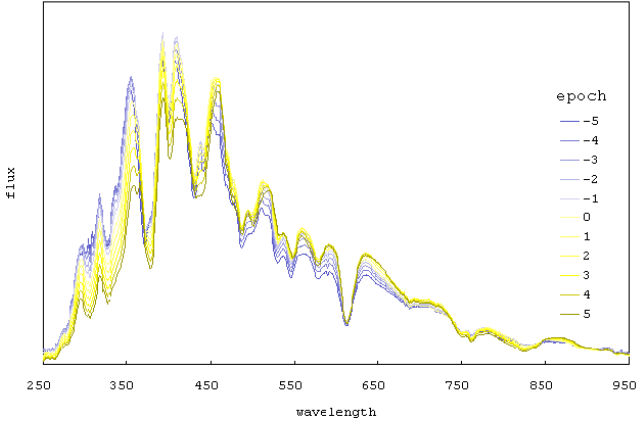


Fig. 6. Type Ia supernovae template

Figure 4 and Figure 5 illustrate the effects different theoretical source spectra have on the shapes of K-corrections. In Figure 4, blackbody spectra of different temperatures are used as the source spectra. The resulting K-corrections show that the colour of the source spectra controls the slopes of the K-corrections. In Figure 5, blackbody spectra with synthetic features were used as the source spectra. Absorption lines at high frequencies in the source spectra are amplified at high redshifts in the resulting K-corrections. Absorption lines at low frequencies are less prominent.

We have demonstrated with theoretical blackbody curves that the shape of the K-correction relies heavily on the spectral shape of the source. An accurate and complete set of source spectra is therefore important. A Type Ia supernovae template is created to cover all wavelengths and epochs by compiling together the colours and the shapes of the observed supernovae spectra (Nugent et al. 2002). A sample of the supernovae template is shown in Figure 6.

A typical K-correction $K_{g'r'}$, calculated using the type Ia supernovae template, is shown in Figure 7. The slope change with epoch in the K-correction corresponds to the supernova spectral colour change. The features in the K-correction correspond to the absorption lines in the supernovae spectra.

2. Filter bands of SDSS and Johnson-Cousins photometric systems

The CFHT Legacy Survey uses the MegaPrime imager. The MegaPrime imager adopts the SDSS photometric system, with filter bands u^* , g' , r' , i' , and z' , shown in Figure 8. MegaCam is the detector of the MegaPrime imager. The quantum efficiency of MegaCam is plotted in Figure 8 as a dashed line. The combined effective transmission of the filters and the detector is also plotted in the same figure.

On the other hand, the CFH12K imager uses filter bands B , V , R , and I in the traditional Johnson-Cousins photometric system. The CFH12K filter set is plotted in Figure 9 and is used for comparison.

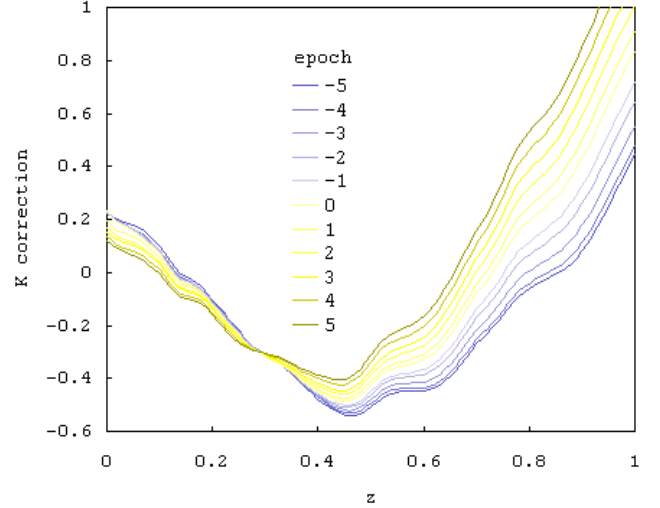


Fig. 7. K-correction $K_{g'r'}$ calculated using the Type Ia supernovae template

MegaPrime		CFH12K	
Filter Bands	λ_{eff} (nm)	Filter Bands	λ_{eff} (nm)
u^*	379	B	438
g'	481	V	538
r'	620	R	656
i'	758	I	807
z'	881	z'	913

Table 1. Effective wavelength of each filter band

The effective wavelength of each filter band, tabulated in Table 1, is calculated using the definition in Schneider et al. (1983):

$$\lambda_{eff} = \exp\left(\frac{\int \lambda^{-1} \ln(\lambda) S(\lambda) d\lambda}{\int \lambda^{-1} S(\lambda) d\lambda}\right)$$

This definition yields a value which approximates the average value obtained using the usual definitions of the effective wavelength and the effective frequency.

This paper uses the filter transmission data of these two imagers for comparison. The relative locations of the filter bands are plotted in Figure 10.

It should again be noted that the relative amplitudes of the filter-detector transmissions are irrelevant. The effective wavelength and the filter bandwidth are the most important properties of a filter-detector transmission in K-correction calculations.

There are relatively large uncertainties in the determining the quantum efficiencies of the detectors. The detector quantum efficiency essentially shifts the effective wavelengths of filter bands u^* and z' , but has minimal effects on filter bands g' , r' , and i' . The uncertainties in the detector quantum efficiency therefore affects $K_{u'z'}$ more than $K_{g'i'}$, as illustrated in Figure 11.

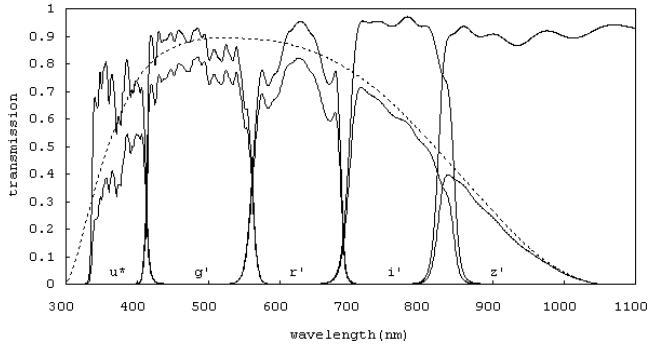


Fig. 8. MegaPrime filter transmissions and detector quantum efficiency

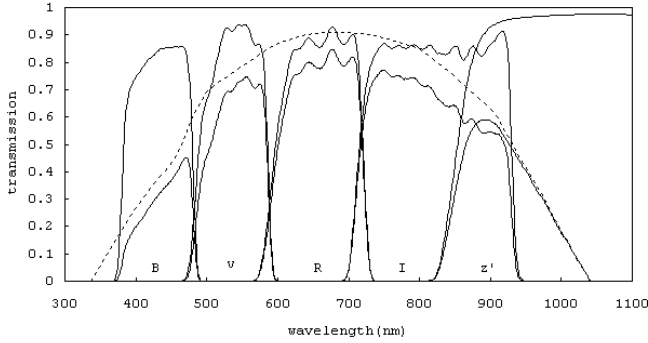


Fig. 9. CFH12K filter transmissions and detector quantum efficiency

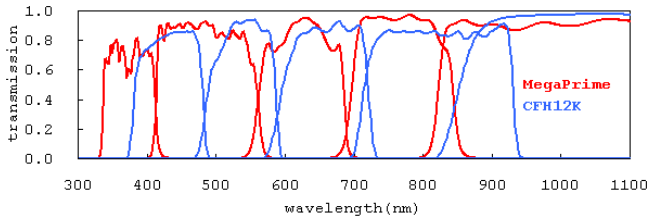


Fig. 10. Wavelength coverages of MegaPrime and CFH12K filter bands

3. Zero magnitude spectra of SDSS and Johnson-Cousins photometric systems

SDSS and Johnson-Cousins are very different photometric systems. As shown in the previous section, their filter sets have very different wavelength coverages. The most important difference between these two photometric systems is the definitions of their system zero magnitudes. The definition of zero magnitude is essential for determining a cross-system K-correction.

The zero magnitude of the Johnson-Cousins system is based on the spectrum of Vega. The U , B , V , R , and I magnitudes are approximately zero for Vega.

The zero magnitude of the SDSS system, on the other hand, is designated by the AB magnitude system of Oke & Gunn (1983):

$$AB_V = -2.5 \log f_V - 48.60$$

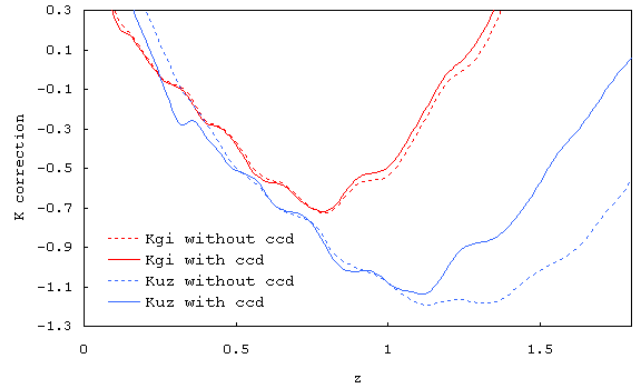


Fig. 11. Effects of uncertainties in detector quantum efficiency

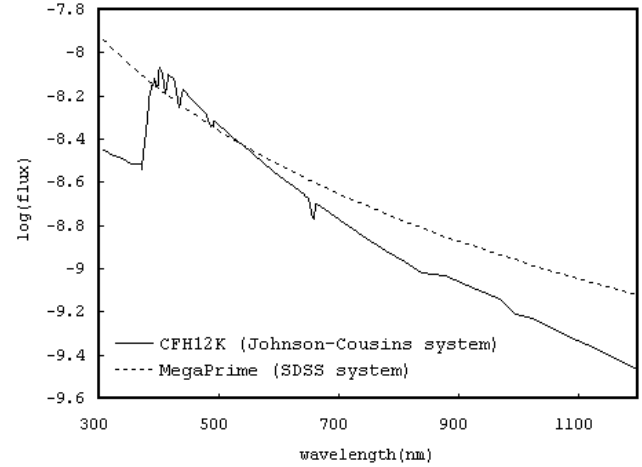


Fig. 12. Zero magnitude spectra of SDSS and Johnson-Cousins systems

At zero magnitude, the AB magnitude system gives a constant and absolute frequency flux:

$$f_\nu = 3.63(10^{-20}) \text{ erg/cm}^2/\text{s/Hz}$$

One can obtain the relative amplitudes of the zero magnitude spectra for the two photometric systems using the absolute flux of the AB magnitude system and the absolute flux of Vega, as illustrated in Figure 12. The knowledge of the zero magnitude spectra allows us to compute cross-filter K-corrections with the rest-frame x and the observed y filter bands in different photometric systems.

4. Convergent point

Every set of K-corrections has a convergent point like the one at redshift z_0 shown in Figure 13. Convergent points occur at redshifts where the rest-frame x and the observed y filter bands are well matched. The location of the convergent point can be approximated by the ratio of the effective wavelengths:

$$\frac{\lambda_{eff-y}}{\lambda_{eff-x}} = 1 + z_0$$

In Figure 13, the K-correction $K_{g'i'}$ was plotted. Filter bands g' and i' are matched at $z_0 = 0.58$, as shown in Figure 14.

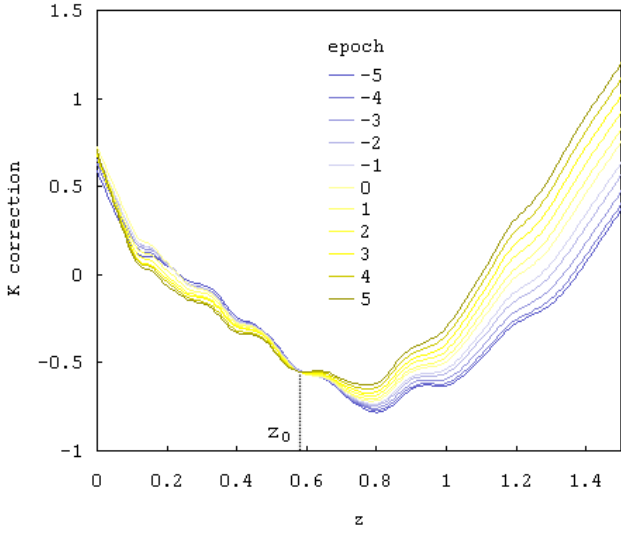


Fig. 13. K-correction $K_{g'i'}$. The redshift z_0 locates the convergent point.

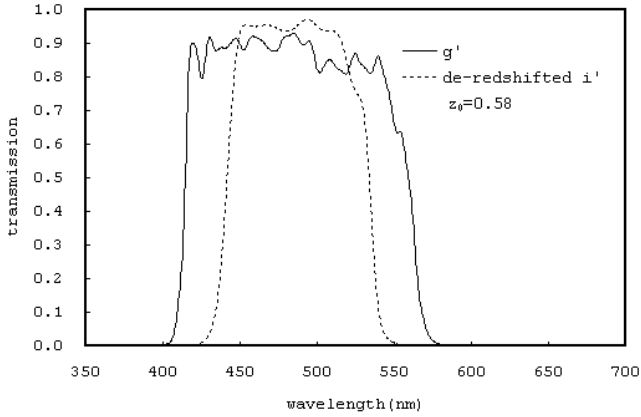


Fig. 14. g' and i' filter are matched at $z = z_0$

At the convergent point, K-correction becomes almost independent of the source spectra. The uncertainties in the source spectral template are consequently minimized at this redshift. This combination of filter bands is therefore ideal for the calculation of K-correction of supernovae at redshift z_0 .

5. Comparing Johnson B and SDSS g' filter bands

In this section, the Johnson B and the SDSS g' filter bands are compared as the rest-frame filter bands. Figure 15 shows that the locations of the two filter bands are in close proximity. The B and g' filter bands are matched at a low redshift. The cross-filter K-correction $K_{Bg'}$ should then reach its minimum at this low redshift, as confirmed by Figure 16.

When the observed y band chosen is the same for the two sets of K-corrections, the K-corrections have the same shape in redshift space. Specifically, K-corrections K_{By} and $K_{g'y}$ would differ by a constant magnitude. To determine this constant mag-

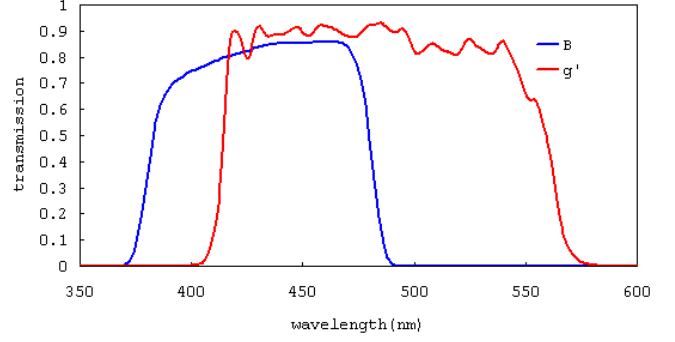


Fig. 15. Johnson B and SDSS g' filter transmissions

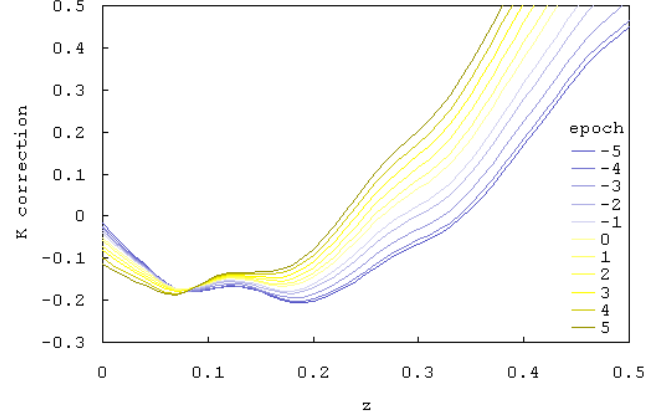


Fig. 16. K-correction $K_{Bg'}$

nitude difference, we refer back to the definition of the cross-filter K-correction:

$$K_{By} - K_{g'y} = -2.5 \log \left(\frac{\int \lambda F(\lambda) S_B(\lambda) d\lambda}{\int \lambda F(\lambda / (1+z)) S'_g(\lambda) d\lambda} \right)$$

The magnitude difference is shown to be the negative of the supernovae colour $B - g'$. The values of $B - g'$ are tabulated in Table 2 and plotted in Figure 17. The shape of the K-corrections K_{By} and $K_{g'y}$ would be dictated by the y band chosen when the same supernovae template is used for all the calculations.

Figure 18 compares the K-corrections K_{By} and $K_{g'y}$ in the zeroth epoch and demonstrates that K_{By} and $K_{g'y}$ have the same shape with a constant magnitude difference of 0.051. For an SDSS observed y filter band, one can convert from the SDSS K-correction $K_{g'y}$ to a cross-system K-correction K_{By} , simply by obtaining the colour $B - g'$ for each epoch of the supernovae spectra.

It should be noted that even though the difference in K-corrections is closely related to colours, generally

$$K_{AB} - K_{BC} \neq K_{AC}.$$

Different choices of the observed y band would yield K-corrections of different shapes. The constant magnitude difference simplification between the two K-corrections is only valid at the redshift $z=0$.

t	$B-g'$																
-19	-0.093	-9	-0.031	1	0.059	11	0.239	21	0.533	31	0.565	41	0.488	51	0.417	61	0.357
-18	-0.093	-8	-0.012	2	0.072	12	0.265	22	0.564	32	0.556	42	0.482	52	0.412	62	0.352
-17	-0.093	-7	0.003	3	0.082	13	0.287	23	0.580	33	0.541	43	0.477	53	0.407	63	0.347
-16	-0.071	-6	0.011	4	0.100	14	0.318	24	0.606	34	0.534	44	0.471	54	0.402	64	0.341
-15	-0.04	-5	0.018	5	0.115	15	0.350	25	0.621	35	0.526	45	0.458	55	0.397	65	0.336
-14	-0.012	-4	0.025	6	0.135	16	0.380	26	0.613	36	0.519	46	0.452	56	0.387	66	0.331
-13	-0.038	-3	0.030	7	0.157	17	0.410	27	0.605	37	0.513	47	0.445	57	0.382	67	0.321
-12	-0.047	-2	0.035	8	0.178	18	0.445	28	0.591	38	0.507	48	0.438	58	0.378	68	0.315
-11	-0.051	-1	0.040	9	0.200	19	0.475	29	0.582	39	0.496	49	0.433	59	0.372	69	0.310
-10	-0.044	0	0.051	10	0.222	20	0.506	30	0.572	40	0.492	50	0.422	60	0.368	70	0.305

Table 2. Colour $B-g'$ of the Type Ia supernovae template

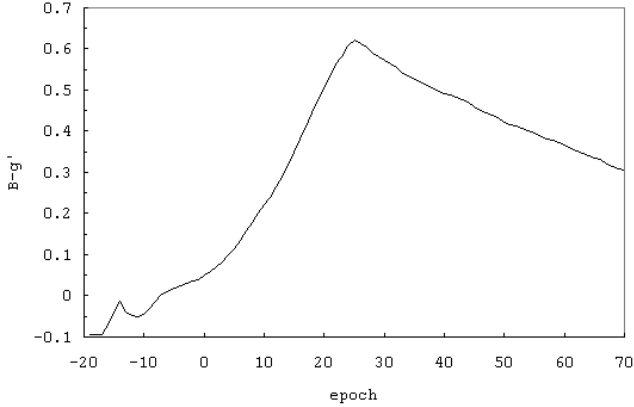


Fig. 17. Colour $B-g'$ of the Type Ia supernovae template

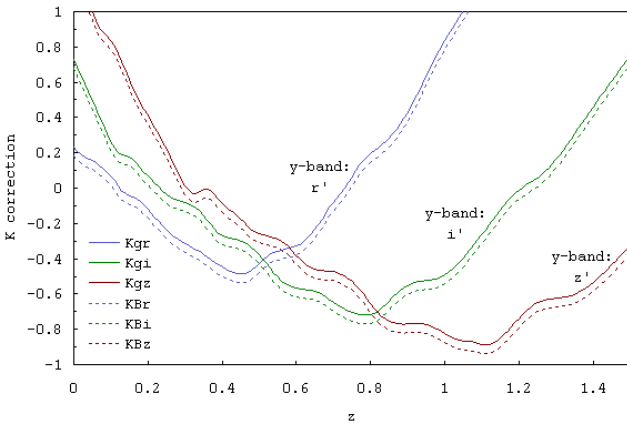


Fig. 18. Comparing K-corrections K_{B_i} and $K_{g'y}$

References

- Cousins, A. W. J. 1978, VRI Photometry of E and F Region Stars, Monthly Notes of the Astronomical Society of South Africa, 37, 8
- Fukugita, M., Ichikawa, T., Gunn, J. E., et al. 1996, The Sloan Digital Sky Survey Photometric System, AJ, 111, 1748
- Johnson, H. L. & Morgan, W. W. 1953, Fundamental stellar photometry for standards of spectral type on the revised system of the Yerkes spectral atlas, ApJ, 117, 313
- Nugent, P., Kim, A., & Perlmutter, S. 2002, K-Corrections and Extinction Corrections for Type Ia Supernovae, PASP, 114,

803

- Oke, J. B. & Gunn, J. E. 1983, Secondary standard stars for absolute spectrophotometry, ApJ, 266, 713
- Robertson, H. P. 1938, The apparent luminosity of a receding nebula. Mit 3 Abbildungen., Zeitschrift fur Astrophysics, 15, 69
- Sandage, A. R., Kron, R. G., Longair, M. S., Binggeli, B., & Buser, R. 1995, The Deep Universe (Saas-Fee Advanced Course 23. Lecture Notes 1993. Swiss Society for Astrophysics and Astronomy, XIV, 526 pp. 204 figs.. Springer-Verlag Berlin Heidelberg New York)
- Schneider, D. P., Gunn, J. E., & Hoessel, J. G. 1983, CCD photometry of Abell clusters. I - Magnitudes and redshifts for 84 brightest cluster galaxies, ApJ, 264, 337